ACTA STEREOL 1994; 13/2: 311-316
PROC 6ECS PRAGUE, 1993
ORIGINAL SCIENTIFIC PAPER

FRACTALITY AND POLYDISPERSITY IN MICROSTRUCTURE OF SILICON NITRIDE CERAMICS

Helmut Hermann[a], Marion Bertram[a], Albrecht Wiedenmann[b] and Matthias Herrmann[c]

[a]Institute of Solid State Research and Materials Science, IFW Dresden, e.V., Postfach, D-01171 Dresden, Germany
[b]Hahn-Meitner Institute Berlin GmbH, Glienicker Str. 100, D-14109 Berlin, Germany
[c]Fraunhofer Institution of Ceramics Technologies and Sintered Materials, (IKTS), Winterbergstr. 28, D-01277 Dresden, Germany

ABSTRACT

A variable model for random two-phase structures with arbitrary volume fraction is presented. The model is capable of creating both fractal and non-fractal polydisperse arrangements. It is used to analyze experimental data on the microstructure of dense silicon nitride ceramics investigated by means of scanning electron microscopy and small-angle neutron scattering.

KEYWORDS: ceramics, fractals, image analysis, small-angle scattering.

INTRODUCTION

High technology ceramics such as silicon nitride offers a series of possible applications where considerable mechanical load capacity is required under high temperature and corrosive conditions. A typical example is the ceramic turbocharger operating at temperatures between 900°C and 1000°C and a speed of more than 10^5 revolutions per minute. Petzow (1990), Ziegler (1989) and Aldinger and Böcker (1992) reviewed the present state of production, characterization, properties, applications and new prospects of high technology ceramics. The microstructure of dense Si_3N_4 ceramics is essentially a two-phase arrangement of rod-like Si_3N_4 particles (about 90 vol%) and a grain boundary phase ranging from intergranular films 1-2nm thick to regions of crystalline oxynitrides of diameter of about 100nm. The grain boundary phase may consist of, e.g., SiO_2, Al_2O_3 and oxides of rare earth elements. It is well known that the thermo-mechanical properties depend strongly on microstructural parameters of the material (Ziegler, 1989), for example on the aspect ratio of the Si_3N_4 particles, and the atomic short-range order and the geometrical distribution of the grain boundary phase.

In the present paper we use a variable model for the geometrical distribution of the grain boundary phase. The model is based on a random set generated by the union of n subsets, and $n \to \infty$, where each subset is a Boolean germ-grain model. The corresponding mathematical body has been summarized by Stoyan et al (1987). The model is capable of creating both fractal and non-fractal polydisperse arrangements. If the model parameters are chosen to produce a surface fractal, the dimension, d_f, of the internal surface may be

varied within the range $2 < d_f < 3$. The covariance (Hermann, 1991) and the chord length distribution function (Hermann and Ohser, 1993), and their variation with well-defined structure parameters are given by analytical expressions. Therefore, the model can be used to analyze experimental data on a certain class of random microstructures and to interprete the data quantitatively in terms of the model parameters. In the present paper this is done for a sample of dense silicon nitride ceramics.

MATERIAL AND METHODS

The sample was produced by hot pressing of Si_3N_4 particles plus 9.3weight% sintering aids. The sintering aids consisted of 82weight% R_2O_3 where R denotes rare earth elements, and 18weight% Al_2O_3, and had been homogenized by chemical methods. The density of the sample is 3.29 g/cm^3, and the volume fraction of pores is well below 1%. The strength is about 980 MPa at room temperature and 560 MPa at 1200°C.

Two quite different experimental methods are employed for the microstructural analysis: Scanning electron microscopy (SEM) and image analysis of the SEM patterns, and neutron small-angle scattering (SANS). For the SEM investigations the sample was ground and polished mechanically and subsequently etched by reactive sputtering. Then, the surface of the sample was covered by a Ag/Pd layer (3nm thick). We used a DSM 962 scanning electron microscope at an accerelation voltage of 10keV. The images were obtained from secondary electrons at magnifications m, $5.000 \leq m \leq 40.000$ The images were taken from arbitrary regions for $m \leq 10.000$ whereas for $m > 10.000$ one had to look for sections exhibiting distinct microstructural details, that means, the observed sections should not be situated within large and homogeneous Si_3N_4 particles. The SEM patterns were transmitted electronically to an QTM 570 image analysis system. There, binary images were generated from the SEM patterns using an automatic grey threshold routine ("auto detect"), and subjected to an erosion procedure with a square structuring element consisting of 9 pixels. Subsequently, the linear contact distribution function of each image was estimated. For definition of that function see Stoyan et al (1987). The corresponding image analysis routine including minus-sampling edge effect correction (Stoyan et al, 1987, p 127) is described by Wendrock and Hübel (1993). As a result, we obtained experimental data for mean volume fraction, $V_V(m)$, mean value, $\bar{l}(m)$, and distribution, $f_m(l)$, of chord length, l, for both the Si_3N_4 particles and the grain boundary phase regions.

The samples prepared for the SANS experiments had the shape of a platelet of thickness 200μm and diameter of about 10mm. The scattering experiments were carried out at the diffractometer PAXY at Laboratoire Leon Brillouin at Saclay. The scattering intensity was recorded in the q-range ($q = 4\pi \sin\Theta/\lambda, 2\Theta$ - scattering angle, λ - wavelength of the neutrons) $1.5 \cdot 10^{-2} nm^{-1} \leq q \leq 2nm^{-1}$ and the irradiated volume was about 5mm^3. The normalized scattering intensity, $I(q)$, is related to the covariance, $C(r)$, by

$$I(q) = 4\pi \int_0^\infty r^2 [C(r) - c^2] \frac{\sin(qr)}{qr} dr \qquad (1)$$

where c is the volume fraction of the regions described by $C(r)$, i.e. either Si_3N_4 particles or grain boundary phase.

The experimental data were analyzed in terms of a random set model A given by the union of subsets A_n

$$A_n = \cup_{i=1}^{\infty} (a_{n,i} + x_i), \quad n = 0, 1, \ldots \qquad (2)$$

which are supposed to be Boolean models. That means the random points, x_i, form a Poisson point field with number density λ_i, and the $a_{n,i}$ are the grains with mean linear size $\overline{b}_n$ (e.g. mean breadth, mean chord length). We generate

$$A = A_0 \cup A_1 \cup ... \cup A_{k-1} \cup A_k ... \cup A_l \cup A_{l+1} \cup ... \tag{3}$$

where

$$\overline{b}_{n+1} = \alpha \overline{b}_n, \quad 0 < \alpha < 1; \quad \lambda_{n+1} = \beta \lambda_n, \quad \beta > 1 \tag{4}$$

and assume A to simulate the distribution of silicon nitride in the sample.

Making use of a given experimental method microstructural details are detected only within a certain range of spatial resolution, r. Considering the model parameters $\overline{b}_k$ and $\overline{b}_l$ defined by Eqs.(2 to 4) to be estimates for the respectively upper and lower limit of r, the experimental data must be compared to the sectional model

$$A_{kl} = A_k \cup A_{k+1} \cup ... \cup A_{l-1} \cup A_l. \tag{5}$$

RESULTS

We took 5, 10, 10 and 15 SEM patterns at magnification 5.000, 10.000, 20.000 and 40.000, respectively, from representative regions of the sample. Fig.1 shows typical images.

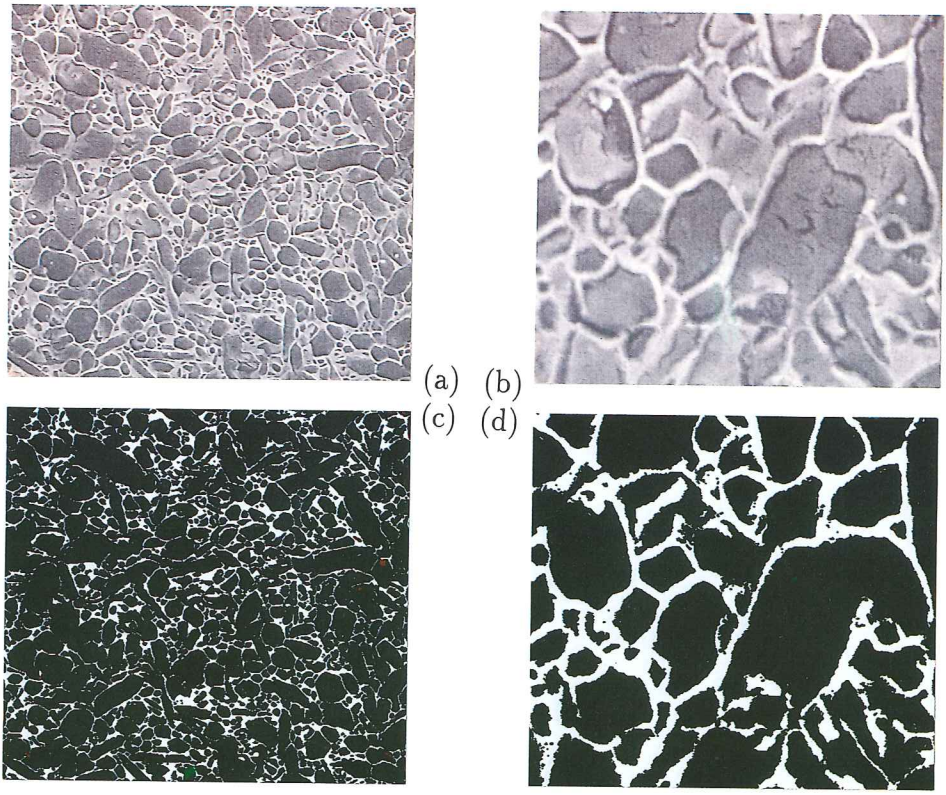

Fig.1. Scanning electron micrographs of silicon nitride, width view $10\mu m$ (a) and $2.5\mu m$ (b), and the corresponding binary images, (c) and (d).

The attribute "representative" means that as much as possible structural details of the grain boundary phase distribution should be visible on each SEM pattern. This is tantamount to the condition that the maximum size of silicon nitride particles visible in the pattern should be small compared to the width view of the pattern. We use the 90% quantile of the silicon nitride chord length distribution as a measure for the maximum size of the observed Si_3N_4 particles. (The γ-quantile Q_γ of a continuous distribution function $F(x)$ is the value Q_γ, with $F(Q_\gamma) = \gamma/100$. That means, a portion $\gamma/100$ of all detected chord lengths has a value less than or equal to Q_γ.) The value l_{90} for a certain magnification is used as an estimate for parameter $\overline{b}_k$ of the sectional model A_{kl}. Parameter $\overline{b}_l$ of A_{kl} is given by the spatial resolution ϵ achieved at magnification m. The results are summarized in Tbl.1.

Now we calculate volume fraction, V_V, and mean chord length, $\overline{l}$, of the complement, A^c_{kl}, of the sectional model A_{kl}. (Remember that A_{kl} is used to simulate the distribution of silicon nitride regions whereas A^c_{kl} is to describe the microstructure of the grain boundary phase.) From the general expressions for Boolean models (Stoyan et al, 1987, pp. 174-180) and the specifications to be made for the present model (see also Hermann, 1991b, pp.31-32, and Hermann and Ohser, 1993) we obtain

$$V_{V,kl} = \exp\{-\lambda_k \overline{V}_k \frac{(\alpha^3\beta)^{l-k} - 1}{\alpha^3\beta - 1}\}, \quad S_{V,kl} = \lambda_k \overline{S}_k V_{V,kl} \frac{(\alpha^2\beta)^{l-k} - 1}{\alpha^2\beta - 1}, \quad \overline{l}_{kl} = 4V_{V,kl}/S_{V,kl}. \tag{6}$$

If $\alpha < \alpha^3\beta < 1$ the model represents a surface fractal with dimension

$$d_f = \begin{cases} -\log\beta/\log\alpha, & \alpha^2\beta > 1 \\ 2, & \alpha^2\beta < 1 \end{cases} \tag{7}$$

of the internal surface (Minkowski-Bouligand dimension, estimated, see Hermann, 1991a). Rewriting Eqs.(6,7) and using the experimental quantities $V_V(m), \overline{l}(m), l_{90}(m), \epsilon(m)$, as estimates for $V_{V,kl}(m), \overline{l}_{kl}(m), \overline{b}_k(m), \overline{b}_l(m)$, respectively, one obtains

$$g_V(m) = \frac{\log V_V(m)}{\log V_{V,0}} = \frac{[l_{90}(m)/b_0]^{3-d_f} - [\epsilon(m)/b_0]^{3-d_f}}{1 - [\epsilon_0/b_0]^{3-d_f}} \tag{8}$$

where the notations $b_0 = \overline{b}_k(5000), V_{V,0} = V_V(5000), \epsilon_0 = \epsilon(5000), \overline{l}_0 = \overline{l}(5000)$ are used. A least-square analysis of the data given in Tab.1 with Eq.(8) yields $d_f = 2.4$.

Analogously to Eq.(8) we define the function $g_l(m)$ and obtain

$$g_l(m) = \frac{\overline{l}(m)}{\overline{l}_0} = \frac{[\epsilon_0/b_0]^{2-d_f} - 1}{[\epsilon(m)/b_0]^{2-d_f} - [l_{90}(m)/b_0]^{2-d_f}}. \tag{9}$$

Again, a least-square fit is carried out. The result is $d_f = 2.5$.

Tbl.1. Results of the image analysis for SEM patterns. m - magnification, w - width view of the image, ϵ - spatial resolution (twice the pixel size), l_{90} - 90% quantile of the chord length distribution of silicon nitride regions, V_V - measured volume fraction of the grain boundary phase, $\overline{l}$ - mean chord length of the grain boundary phase.

m	$w(m)/nm^2$	$\epsilon(m)/nm$	$l_{90}(m)/nm)$	$V_V(m)$	$\overline{l}(m)/nm$
5.000	18432 × 17352	72	1280	0.070	107
10.000	9216 × 8676	36	653	0.136	83
20.000	4608 × 4338	18	412	0.227	65
40.000	2304 × 2169	9	334	0.248	64

We consider now the SANS data shown in Fig.2. The scattering curve corresponding to the present model can be calculated from Eq.(1) with

$$C(r) = 2c - 1 + (1-c)^2 \exp[\lambda\overline{\gamma}(r)] \tag{10}$$

(Stoyan et al, 1987, p.72) where

$$\gamma(r) = \int s(\vec{u}+\vec{r})s(\vec{u})dV_u d\Omega, \quad r = |\vec{r}|, \quad s(\vec{r}) = \begin{cases} 1, & \vec{r} \text{ in } a \\ 0, & \text{otherwise.} \end{cases} \tag{11}$$

Function $s(\vec{r})$ is the so-called shape function of grain a (see Eq.(2)) , $\int ...dV_u$ denotes the integration over all endpoints of vector $\vec{u}$ in space, $\int ...d\Omega$ is the average over all spatial directions, and $\overline{\gamma}$ is the average of γ over all grains contributing to the model defined by Eqs.(2, 3). (For a brief review see Hermann, 1991b, pp. 42-68.) We may simulate the covariance, $C(r)$, for the region covered either by silicon nitride or by the grain boundary phase. For simplicity ($V_V << 1$) we consider the grain boundary phase, expand Eq.(10) in terms of V_V and use random Poisson polyhedra (see Stoyan, 1987, p. 84) to simulate the complement of A by a second Boolean model. Then, the small-angle scattering intensity is given by the explicit formula

$$I(q) = 8\pi V_V(1-V_V) \lim_{n\to\infty} \frac{\alpha^{3-d_f}-1}{\alpha^{(3-d_f)n}-1} \sum_{j=0}^{n-1} \frac{\beta_j \alpha^{(3-d_f)j}}{(\beta_j^2+q^2)^2}, \quad \beta_j = \frac{3}{2\alpha^j b_0} \tag{12}$$

which is used to approximate the experimental curve in Fig.2 and to estimate the model

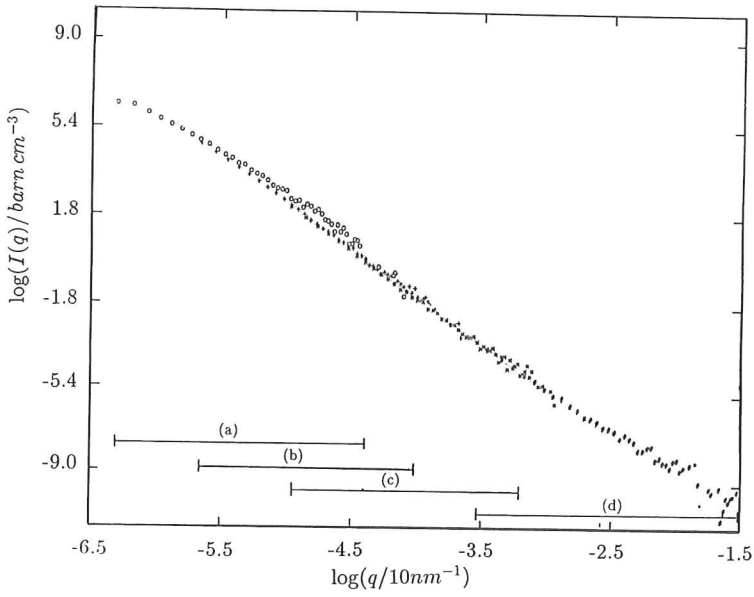

Fig.2. Small-angle neutron scattering curve of silicon nitride obtained at different experimental conditions (wavelength, distance sample-detector): (a) 2nm, 6.84m; (b) 1.2nm, 6.84m; (c) 0.6nm, 6.84m; (d) 0.6nm, 1.5m.

parameters by a least-square fit. The result for the fractal dimension and the maximum size (mean breadth) of the regions covered by the grain boundary phase are reliable and take the values $d_f = 2.4$ and $b_0 = 100$nm.

The least-square routines were stable with respect to variation of starting values for both image analysis and SANS method. The error of d_f was estimated from the mean deviation of experimental data from the fitted curves and was below 5%.

DISCUSSION

The present analysis shows that the distribution of the grain boundary phase in the investigated sample of silicon nitride ceramics is extremely polydisperse. The linear extent of microstructural components ranges from few nanometres detected especially by SANS to more than 1μm. Both SANS and SEM plus subsequent image analysis proved the microstructure to have typical traits of a surface fractal with dimension $d_f = 2.4 \pm 0.1$ of the internal surface. The advantage of the SANS method consists in the accurate average over all microstructural components of the sample. However, one should be sure that the scattering intensity is caused only by the microstructural components under investigation. Furthermore, the analysis of the intensity curve requires a structural model which, in general, cannot be derived from a single scattering curve. The SEM patterns give an immediate image of the microstructure and qualitative features can be found out already by visual inspection. Quantitative estimates, however, require some image analysis and, for statistical reliability, a rather extensive series of individual patterns. Of course, it is recommendable to utilize both complementary methods for microstructural analyses.

For the present investigation it was of great importance to have available a detailed and variable structure model since both the definitions of microstructural parameters and the methods for their estimations have been derived from the model.

REFERENCES

Aldinger F, Böcker WDG. Development of ceramic high performance materials (in German). Keramische Z 1992; 44: 236-240.

Hermann H. A new random surface fractal for applications in solid state physics. Physica Status Solidi (b) 1991a; 163: 329-336.

Hermann H. Stochastic models of heterogeneous materials. Zurich: Trans Tech Publ., 1991b.

Hermann H, Ohser J. Determination of microstructural parameters of random spatial surface fractals by measuring chord length distributions. J Microsc 1993; 170: 87-93.

Petzow G. High-tech ceramics - new materials bring new prospects. In: Kürsten M, ed. Raw materials for new technologies. Stuttgart: Schweizerbart'sche Verlagsbuchhandlung, 1990: 39-55.

Stoyan D, Kendall WS, Mecke J. Stochastic geometry and its applications. Chichester: Wiley & Sons, 1987.

Wendrock H, Hübel R. Characterization of microstructural anisotropies in steel by means of the mathematical morphology. 6th European Congress for Stereology. Prague, September 7-10, 1993; Book of abstracts, p vi-2, and Acta Stereol, present issue.

Ziegler G. Thermo-mechanical properties of silicon nitride and their dependence on microstructure. Mater Sci Forum 1989; 47: 162 - 203.